

# A simple method for the isolation and detailed characterization of primary human proximal tubule cells for renal replacement therapy

The International Journal of Artificial  
Organs  
1–13

© The Author(s) 2019

Article reuse guidelines:

sagepub.com/journals-permissions

DOI: 10.1177/0391398819866458

journals.sagepub.com/home/jao



Natalia Sánchez-Romero<sup>1,2</sup>, Laura Martínez-Gimeno<sup>1,2</sup>,  
Pedro Caetano-Pinto<sup>3,4</sup>, Berta Saez<sup>5,6</sup>, José Manuel Sánchez-Zalabardo<sup>5,7</sup>,  
Rosalinde Masereeuw<sup>3</sup> and Ignacio Giménez<sup>1,2,8</sup> 

## Abstract

The main physiological functions of renal proximal tubule cells *in vivo* are reabsorption of essential nutrients from the glomerular filtrate and secretion of waste products and xenobiotics into urine. Currently, there are several established cell lines of human origin available as *in vitro* models of proximal tubule. However, these cells appeared to be limited in their biological relevance, because essential characteristics of the original tissue are lost once the cells are cultured. As a consequence of these limitations, primary human proximal tubule cells constitute a suitable and a biologically more relevant *in vitro* model to study this specific segment of the nephron and therefore, these cells can play an important role in renal regenerative medicine applications. Here, we describe a protocol to isolate proximal tubule cells from human nephrectomies. We explain the steps performed for an in-depth characterization of the cells, including the study of markers from others segments of the nephron, with the goal to determine the purity of the culture and the stability of proteins, enzymes, and transporters along time. The human proximal tubule cells isolated and used throughout this study showed many proximal tubule characteristics, including monolayer organization, cell polarization with the expression of tight junctions and primary cilia, expression of proximal tubule-specific proteins, such as megalin and sodium/glucose cotransporter 2, among others. The cells also expressed enzymatic activity for dipeptidyl peptidase IV, as well as for gamma glutamyl transferase I, and expressed transporter activity for organic anion transporter 1, P-glycoprotein, multidrug resistance proteins, and breast cancer resistance protein. In conclusion, characterization of our cells confirmed presence of putative proximal tubule markers and the functional expression of multiple endogenous organic ion transporters mimicking renal reabsorption and excretion. These findings can constitute a valuable tool in the development of bioartificial kidney devices.

## Keywords

Proximal tubular cells, human primary culture, isolation, characterization, renal physiology, mimicking, bioartificial kidney

Date received: 24 October 2018; accepted: 8 July 2019

<sup>1</sup>Instituto Aragonés de Ciencias de la Salud (IACS), Zaragoza, Spain

<sup>2</sup>Instituto de Investigación Sanitaria Aragón (IIS Aragón), Zaragoza, Spain

<sup>3</sup>Division of Pharmacology, Utrecht Institute for Pharmaceutical Sciences, Faculty of Science, Utrecht University, Utrecht, The Netherlands

<sup>4</sup>Mechanistic Safety and ADME Sciences, Drug Safety and Metabolism, IMED Biotech Unit, AstraZeneca, Cambridge, UK

<sup>5</sup>Hospital Clínico Universitario Lozano Blesa, Zaragoza, Spain

<sup>6</sup>Universidad San Jorge, Zaragoza, Spain

<sup>7</sup>Hospital Universitario Miguel Servet, Zaragoza, Spain

<sup>8</sup>Department of Pharmacology and Physiology, University of Zaragoza, Zaragoza, Spain

## Corresponding author:

Ignacio Gimenez, Instituto Aragonés de Ciencias de la Salud, Avda. S. Juan Bosco 13, 50009 Zaragoza, Spain.

Email: [igimenez@unizar.es](mailto:igimenez@unizar.es)

## Introduction

Chronic kidney disease (CKD) is a severe health problem that affects around 10%–15% of the adult population worldwide.<sup>1,2</sup> In this disease, the impaired renal function promotes the accumulation of endogenous uremic metabolites.<sup>3,4</sup> The treatment during stages I–IV of CKD is focused on delaying the evolution of the disease, at the same time that preventing or treating all the associated complications. In the final stage of CKD, known as end-stage renal disease (ESRD), renal replacement therapy (RRT) such as dialysis or kidney transplantation is necessary to maintain life in these patients. However, dialysis is insufficient to remove large and protein-bound uremic toxins, and cannot replace active secretion/absorption of metabolites and the endocrine function played by renal tubule cells.<sup>5</sup> Furthermore, organ transplantation is currently affected by a huge organ shortage, as well as graft failure.<sup>6</sup>

One of the most important achievements in the area of kidney regenerative medicine has been the development of bioartificial kidneys (BAKs). This technology represents the intersection between regenerative medicine and RRT.<sup>7</sup>

The term *bioartificial kidney* (BAK) was introduced in 1987 by Aebischer et al.<sup>8</sup> and identifies a system able to support or replace the natural filtrating process of the kidney. A BAK design combines a conventional hemofilter with a bioreactor unit that contains proximal tubule (PT) cells, designated renal assist device (RAD).<sup>9,10</sup> The differences between BAKs developed up to now are based on the supporting membrane and the renal cells used. The biomaterial field has experienced a rapid advancement in the last decade, and currently the availability of materials designated to successfully support cell growth in membranes is diverse. Materials most commonly used are hollow fibers made of polyethersulfone (PES), polyvinylpyrrolidone (PVP), polysulfone (PSF), or their copolymers.<sup>11,12</sup> More importantly, the successful development of a BAK directly depends on the cell source used to replace the transporter function of the kidneys.<sup>13,14</sup> Among the different cell types located in the kidney, the PT cells play a major role in the reabsorption of filtered substances, such as glucose and amino acids,<sup>15</sup> and in the excretion of xenobiotics, such as environmental chemicals, drugs, or endogenous waste products originating from metabolism, by secreting them into the urine.<sup>16,17</sup>

Morphologically, the PT epithelium consists of polarized epithelial cells.<sup>18,19</sup> The apical cell membrane contains a brush border. The cytosol of the PT cells contains a large number of mitochondria reflecting the high levels of energy required to execute their specialized functions. For their secretory role, PT cells are equipped with a range of transporters, consisting of multiple carriers with overlapping substrate specificities that cooperate in basolateral uptake and luminal secretion.<sup>20</sup> For instance,

uptake of organic anions is mediated by members of the solute carrier (*SLC*) family, known as organic anion transporters 1 and 3 (OAT1/3; *SLC22A6* and *A8*) and the bidirectional organic anion transporting peptide 4C1 (OATP4C1; *SLCO4C1*).<sup>21,22</sup> Cellular efflux of organic anions is facilitated by members of the ATP-binding cassette (ABC) transporter family, known as the multidrug resistance proteins 2 and 4 (MRP2/4; *ABCC2* and *ABCC4*), and breast cancer resistance protein (BCRP; *ABCG2*), through ATP-dependent transport.<sup>23,24</sup> In the case of organic cations, the uptake is mediated by *SLCC22* family of organic cation transporters (OCTs), located at the basolateral membrane of PT. At the apical membrane, the *SLC47* multidrug and toxin extrusion (MATE) proteins are expressed.<sup>25,26</sup> ABC transporters permeability (P)-glycoprotein (*ABCB1*; MDR1/P-gp) and the BCRP (*ABCG2*) are also involved in the apical transport of some uncharged and cationic substrates.<sup>27–29</sup> Biochemically, PT cells are characterized by the expression of markers as megalin, sodium/glucose cotransporter 2 (SGLT-2), gamma glutamyl transferase gamma glutamyl transferase 1 (GGT1), dipeptidyl peptidase IV (DPPIV), aminopeptidase M (APM), among others.<sup>30,31</sup>

Taking into account the physiological role played by these cells in vivo, well-characterized PT cell cultures are needed to study different aspects of renal physiology, pharmacology, and for the implementation of these cells in the development of BAKs. Currently, there are several established cell lines of human origin available as in vitro models of PT.<sup>17</sup> These cell lines have the ability to proliferate indefinitely or at least between 20 and 80 passages and are used as a cost-effective tool in basic research. However, these cell lines are less used as a biologically essential tool, basically because important characteristics of the original tissue are lost once the cells are in culture. A good example of a continuous epithelial cell line with altered characteristics compared with the original tissue is the MDCK line (Madin–Darby canine kidney epithelial cells) derived from the kidney of a cocker spaniel. This cell line forms an epithelium in culture, but not a basement membrane, typical for the kidney. This is because MDCK has lost the capability to bring these proteins to the basolateral side of the epithelium in an insoluble form and to interlace them three dimensionally into a functional basement membrane.<sup>32</sup> Primary human PT cells (hPTC) constitute a good in vitro model to overcome the limitations and to study this specific segment of the nephron and more importantly, they constitute a more biologically relevant option. For this reason, many researchers have focused on the development of procedures for the isolation and characterization of hPTC.<sup>33–36</sup>

Here, we have developed a novel protocol for the isolation and phenotypical characterization of proximal tubular cells from healthy human nephrectomies. The hPTC

isolated and used throughout this study showed many characteristics of PT, including monolayer organization, cell polarization with the expression of tight junctions and primary cilia, expression of the specific PT proteins, as megalin and SGLT-2, among others. They also expressed enzymatic activity for DPPIV, as well as GGT1. Moreover, the cells expressed transporter activity for OAT1, P-gp, MRP, and BCRP. Hence, hPTC constitute a powerful tool for the development of BAK applications, as well as in vitro transport studies in pharmacology/toxicology, and studies of renal physiology and pathology.

## Material and methods

### Isolation protocol of human proximal tubular cells

Primary renal cortical cells were isolated from healthy sections of human kidney obtained under patient consent from discarded organs after radical nephrectomies. The procedure was approved by the regional committee on human research (Comité de Ética en Investigación Clínica de Aragón, CEICA).

The protocol used for the isolation of hPTC was adapted from preceding reports in the literature, and consisted of the following steps:

1. Cortical samples were decapsulated and dissected to obtain 1-mm<sup>3</sup> fragments.
2. The resultant fragmented tissue was transferred to a Falcon tube containing ice-cold EBSS (Earle's balanced salt solution) medium (Lonza, Spain) and centrifuged at 4°C, 400 g during 8 min to remove waste material.
3. The fragments were then digested in 6.25 mL of complete EBSS medium with 0.025% collagenase type I (Sigma, Germany), incubated at 37°C for 10 min with continuous agitation and oxygenation.
4. Large pieces of undigested tissue were allowed to sediment before collecting the cell and tubule suspension, which was centrifuged at 1000 g for 10 min, and subsequently, the pellet was resuspended and maintained in ice-cold EBSS medium and 0.2% of bovine serum albumin (BSA; Sigma). Steps 3 and 4 were repeated four times or until all tissue had been digested.
5. Collected cell/tubule suspension in ice-cold EBSS-BSA was sieved through a 100- $\mu$ m cell strainer (to remove undigested tissue and large tubule or aggregates). Material retained by the filter was collected, and was used to start primary cultures. The filtrate was further sieved through a 40- $\mu$ m cell strainer. The resulting filtrate was pelleted at 1000 g for 5 min.
6. Cell suspensions were washed twice in PBS (without Ca<sup>2+</sup>/Mg<sup>2+</sup>) (Lonza, Spain) and centrifuged for 5 min at 500 g.
7. Cells were initially seeded on 6-well plates and cultured with renal complete culture medium (RCM)<sup>37</sup> containing Dulbecco's modified Eagle's medium (DMEM) and Ham's F12, 2% (v/v) fetal calf serum (FCS), 100 units/mL penicillin, 100 units/mL streptomycin, 0.25  $\mu$ g/mL amphotericin, 5  $\mu$ g/mL insulin, 5  $\mu$ g/mL transferrin, 10 ng/mL selenium, 5  $\times 10^{-8}$  M dexamethasone, 10<sup>-9</sup> M tri-iodothyronine (T3), and 10 ng/mL epidermal growth factor (EGF) at 37°C under 5% CO<sub>2</sub> in a humidified atmosphere. The culture medium was renewed after 24 h in order to eliminate non-adherent and residual cells.

### Biobanking of hPTC cells

**Passage and maintenance of hPTC cells.** Cultures of hPTC were subcultured until 80%–90% confluency. First, cells were washed with phosphate buffered saline (PBS; without Ca<sup>2+</sup>/Mg<sup>2+</sup>) and then incubated with 0.25% trypsin (Lonza, BE02-007E) at 37°C in a 5% CO<sub>2</sub> incubator until detached. After that, cells were resuspended in RCM medium to stop the effect of trypsin, centrifuged at 117 g for 5 min and counted using a Neubauer cytometer. Approximately 4000 cells/cm<sup>2</sup> were seeded in each passage. The growth medium was changed twice weekly until confluency was reached. Doubling times were calculated from cell number at seeding and subpassing. Cells were tested for mycoplasma in first passage.

**Cell freezing and thawing.** The cell and tubule suspension used to initiate the primary cultures was designed as P0. First passage (P1) was amplified to obtain a high number of cells, which subsequently were aliquoted and stored frozen under liquid nitrogen. For experimentation purposes, cells were thawed and seeded directly on the selected containers. Freezing and thawing procedures followed standard protocols. Cells were frozen and stored in DMEM supplemented with 20% fetal bovine serum (FBS) and 10% dimethyl sulfoxide (DMSO), at a concentration of 0.5  $\times 10^6$  cells/mL.

### Analysis of phenotypic markers expression by reverse transcriptase–polymerase chain reaction (RT-PCR)

Total RNA was extracted from 25,000 cells growing during 7 days in each cellular passage, following manufacturer instructions (RNA Purification; Norgen Biotek, Canada), and concentrations were determined using a NanoDrop spectrophotometer (Thermo Sci, Spain). RNA transcripts were retrotranscribed into cDNA through the

**Table 1.** Primers used in RT-PCR multiplex analysis.

Mix	Marker	Primers sequences	Amplicon	Information provided
1	Megalin	F: CATCCCAAGCGAATGGATCTG R: CAGTACAATCCACATCGCCATC	185 bp	PT brush border protein
	KSP	F: TCCCATGCCTACCTCACCTT R: TTGCAGCGACACACGATCA	125 bp	Renal epithelial cadherin
	DPPIV	F: TACTACTGGCTGGGTTGGAAG R: TGTCTGTAACCTTCTTCATTGCTG	102 bp	PT brush border enzyme
2	APN	F: GAACGATCTCTTGAGCACATGAG R: GAAGAGGGTGTGTTTCAGCG	232 bp	PT brush border enzyme
	GAPDH	F: TTGACGCTGGGGCTGGCATT R: GTGCTCTTGCTGGGGCTGGT	157 bp	Endogenous control
	GGT1	F: TGAGCCCAGAAGTGAGAGCAGTTG R: ATGTCCACCAGCTCAGAGAGGGT	85 bp	PT brush border enzyme
3	THP	F: GAGTGTCACCTGGCCTACTG R: CATGGGTTTCATTCTCGTCAAC	358 bp	TAL luminal protein
	ASMA	F: CTACAATGAGCTTCGTGTTGCC R: GCGTCCAGAGGCATAGAGAG	172 bp	Myofibroblast
	SGLT-2	F: ACGCCTGATTCCCGAGTTCT R: AGAACAGCACAAATGGCGAAGT	110 bp	PT glucose transporter
4	AQP-2	F: ATCACGCCAGCAGACATCC R: AGCACGTAGTTGTAGAGGAGGG	350 bp	CD water channel
	NKCC2	F: TGGGGAGTCATGCTCTTCATTTCG R: CCACGAACAAACCCGTTAGTTGC	149 bp	TAL sodium transporter
	NCC	F: CACCAAGAGGTTTGAGGACATG R: GACAGTGGCCTCATGCCTTGAA	70 bp	DT sodium transporter

PT: proximal tubule; KSP: kidney-specific cadherin; DPPIV: dipeptidyl peptidase IV; APN: aminopeptidase N; GAPDH: glyceraldehyde-3-phosphate dehydrogenase; GGT1: gamma glutamyl transferase; TAL: thick ascending limb; SGLT-2: sodium/glucose cotransporter 2; CD: collecting ducts.

commercial kit High-Capacity cDNA Reverse Transcription Kit (4387406; Applied Biosystems, Spain) according to manufacturer's instructions. First, primers were validated for each individual marker, using RNA from unprocessed human kidney tissue, under same PCR conditions (buffers, magnesium, cyclor settings). RT-PCR was set up using the commercial kit DSF-Taq (Bioron, Germany). After an initial denaturation step at 94°C for 2 min, 40 cycles of 45 s at 94°C, 30 s of hybridization at 62°C, and 1.30 min of extension at 72°C were carried out. A final extension period of 5 min was performed at 74°C. RT-PCR products were loaded onto 2% agarose gels, stained with ethidium bromide and visualized under a G:BOX (Syngene, Spain) with an ultraviolet light integrated.

For multiplex PCR, four sets of three markers each were developed. Phenotypic markers were grouped to allow size discrimination of the amplicons (covering the 70–400 bp range). Markers included in the mixes represent phenotypes of interest: renal epithelium (kidney-specific (KSP) cadherin), PT (GGT1, megalin, aminopeptidase N (APN), SGLT-2, DPPIV), and markers of dedifferentiation or contamination (aSMA, THP, NKCC2, NCC, AQP2). Mix 3 included an internal

control (glyceraldehyde-3-phosphate dehydrogenase (GAPDH)) (Table 1).

### Immunofluorescence

The hPTC were seeded at a density of 8000 cells/cm<sup>2</sup> on glass coverslips and cultured until confluence was reached. The hPTC monolayers were fixed by using 4% paraformaldehyde, permeabilized in 0.2% Triton X-100 and incubated in a quenching solution (50 mM NH<sub>4</sub>Cl). Afterward, cells were incubated with the blocking solution (phosphate-buffered saline (PBS), 0.1% Tween 20, 0.1% BSA, and 10% goat serum) and then with antibodies against the tight junction protein zonula occludens 1 (ZO-1) (1:40; Santa Cruz Biotechnology, Spain) and acetylated tubulin (1:1000; Sigma), following incubation with secondary goat anti-rabbit-Alexa 488 (1:1000; Invitrogen, Spain) or goat anti-mouse-Alexa 555 (1:1000; Invitrogen). Coverslips were mounted in Vectashield Hard Set™ Mounting Medium (H-1400; VectorLabs, UK) supplemented with 4,6-diamidino-2-phenylindole (DAPI) (1:1000; Molecular Probes, Invitrogen). Images were taken using an Olympus IX81 inverted fluorescence microscope. Full image

brightness and contrast adjustments and channel overlays were produced by using Photoshop (Adobe, USA) and ImageJ.

### **Immunocytochemistry**

About 8000 cells/cm<sup>2</sup> were plated on glass coverslips and maintained until reaching confluence. The hPTC cell monolayers were fixed with 4% paraformaldehyde and permeabilized with 0.1% Triton X-100. Endogenous peroxidase activity was quenched by incubating the sample with 3% H<sub>2</sub>O<sub>2</sub>. Non-specific binding sites were blocked by incubation with PBS and 1 drop of normal goat serum from Vectastain Elite ABC kit (VectorLabs), and cells were incubated with primary antibodies diluted in blocking solution: GGT1 (1:50; Abcam, USA), megalin (1:50; SantaCruz Biotechnology, Spain), calbindin 28 (CB-28) (1:50; Sigma), and alpha smooth muscle actin ( $\alpha$ -SMA) (1:50; Sigma). Control samples were incubated in the absence of primary antibody. Following treatment with biotinylated secondary antibodies (1:200; VectorLabs), cells were incubated with Vectastain Elite ABC kit (VectorLabs) and Sigmafast DAB kit (Sigma). Cells were counterstained with hematoxylin-eosin (VectorLabs) and mounted in Vectashield Hard Set<sup>TM</sup> Mounting Medium (H-1400; VectorLabs). Images were taken using an Olympus IX81 inverted microscope. Control and stained source images acquired in the same session were merged into a single image file, in which brightness and contrast was adjusted by using Photoshop (Adobe).

### **Flow cytometry**

Confluent hPTC monolayers were washed twice with PBS and trypsinized. The  $5 \times 10^5$  live cells were labeled with PE-conjugated anti-CD13 (Acris, Germany), FITC-conjugated anti CD26 (Acris), and APC-conjugated anti-CD10 (Immunostep, Spain), CD13<sup>+</sup> (Acris) in 50  $\mu$ L of PBS. Cells were pelleted by centrifugation and stained with propidium iodide to determine cell viability. The labeled cells were analyzed using a flow cytometer (BD FACSAria).

### **Determination of enzyme activity in live cultured cells**

GGT1 and DPPIV enzymatic activities were determined by measuring the release of p-nitroaniline from specific enzyme substrates. GGT1 activity was assessed using 2 mM  $\gamma$ -glutamyl-p-nitroanilide (GGpN; Sigma) and 50 mM glycylglycine (Sigma) in 1 mL HBSS (Hank's balanced salt solution). DPPIV activity was determined using 1 mM Gly-Pro-p-nitroanilide (GPpN; Sigma) in 1 mL

HBSS. The hPTC growing in 96-well plates were incubated in the presence of enzyme substrates during 1 h at 37°C in a plate reader, set to record absorbance at 405 nm every 20 min. The results were expressed as mmol p-nitroaniline/h/cm<sup>2</sup>.

### **Drug transporter assays**

The hPTC were seeded at a density of 8000 cells/cm<sup>2</sup> in 96-well plates and maintained at 37°C in a 5% CO<sub>2</sub> atmosphere during 7 days until confluence was reached. To determine the uptake by the OAT1 transporter, cells were incubated with 5  $\mu$ M fluorescein (Sigma) during 40 min at 37°C. To inhibit OAT1 transporter, cells were pre-incubated using 100  $\mu$ M probenecid (Sigma) during 15 min, followed by incubation with the inhibitor and fluorescein (5  $\mu$ M) during 40 min at 37°C. After the incubation, cells were washed with HBSS buffer, lysed in 0.1 M NaOH under shaking for 20 min. Fluorescence was measured in a plate reader at 485 nm of excitation and 535 nm of emission. The same procedure was used to determine the activity of BCRP, but with Ko143 (15  $\mu$ M) to inhibit efflux before acquiring fluorescence.

The activity of ABC efflux transporters P-gp and MRP was determined by measuring the accumulation of the typical cell viability substrate calcein (Sigma).<sup>38</sup> Cells were incubated with 1.25  $\mu$ M calcein-AM in the presence or absence of the inhibitors PSC-833 (6  $\mu$ M; Tocris, UK) or MK571 (50  $\mu$ M; Tocris) at 37°C for 40 min. Then, cells were washed with HBSS buffer and lysed with a solution containing 1% Triton X-100. The resulting fluorescence was measured in a plate reader at 488 nm of excitation and 518 nm of emission.

### **Data analysis**

All experiments were performed at least in three independent replicates. Data are expressed as mean  $\pm$  SD of multiple replicates. Statistical analysis was performed using two-tailed Student's t-test in Microsoft Excel. Differences between groups were considered to be statistically significant when  $p < 0.05$ .

## **Results**

### **Evolution of hPTC morphology through subcultivation**

All kidney samples from nephrectomies processed to isolate PT cells contained viable single cells with the ability to proliferate into cell colonies and eventually form a confluent cell monolayer. Small colonies were formed 2–3 days after isolation (Supplementary Figure 1). To reach a confluent cell monolayer, cells needed to grow on

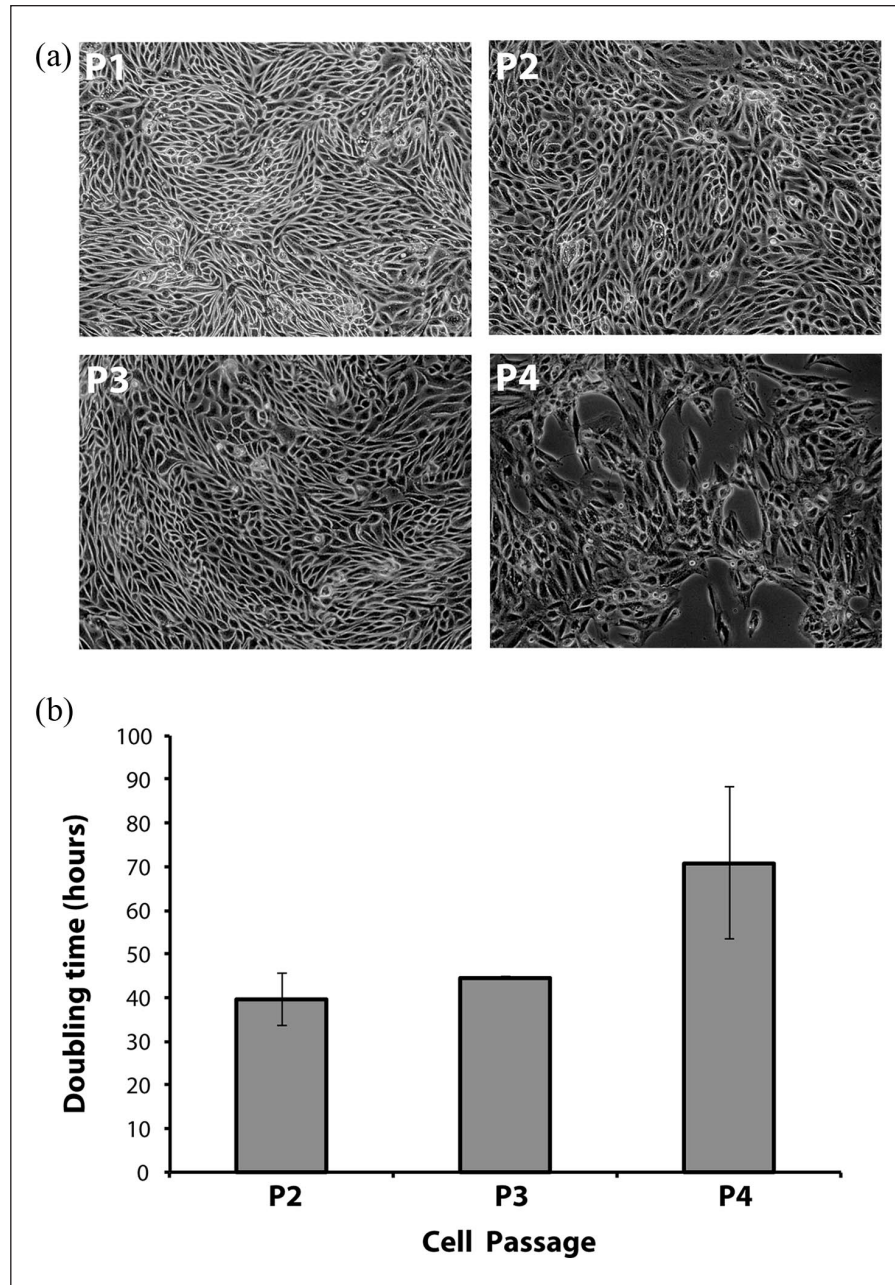


**Figure 1.** Morphology progression and doubling time in cultured hPTC. (a) Representative phase contrast images of primary cells in passage 1 (P1), passage 2 (P2), passage 3 (P3), and passage 4 (P4). Cells maintained epithelial morphology and form a characteristic monolayer till passage 3. (b) Doubling times of hPTC over passages were calculated from cell numbers at seeding and subculturing and are expressed in hours (mean  $\pm$  SD, n=3).

average approximately 7 days for each passage. Primary cultures showed the typical cobblestone appearance of epithelial cells in passages 1, 2, and 3 and a heterogeneous morphology in passage 4 (Figure 1(a)). Doubling time expressed in hours was determined for each passage number, showing an increase dependency per cell passage (Figure 1(b)).

#### *Transcriptional expression of phenotypic markers in hPTC*

The phenotype of the isolated hPTC was evaluated by using multiplex RT-PCR. In this study, multiplex PCR applied analyzed 12 reactions combined in 4 mixes of 3 targets each; an endogenous control was included. The

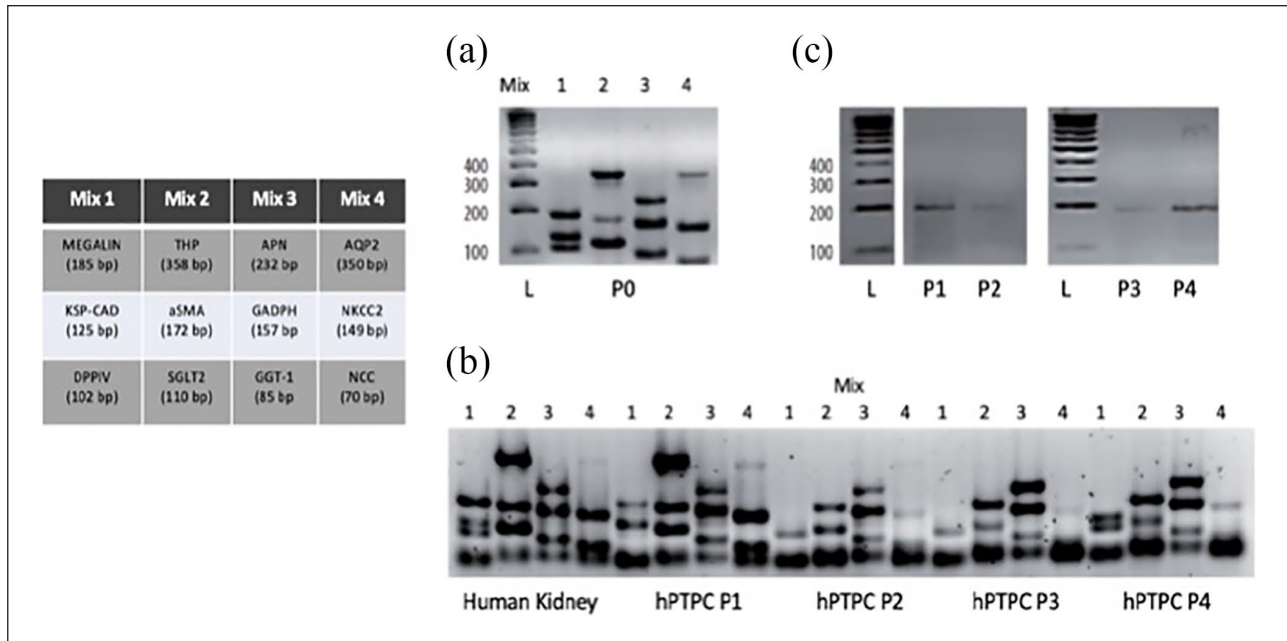


**Figure 2.** Transcriptional profiling by multiplex RT-PCR. The box on the left represents the combination of markers used in each mix analyzed. (a) Analysis of starting material (P0) shows the expression of markers of cortical nephron segments (L: Ladder). (b) Expression of markers across passages 1–4. RNA from whole human kidney was used as control. PT markers were present from passage 1 to passage 4, along with markers from other nephron segments as NKCC2 and NCC. (c) Individual RT-PCR analysis for megalin shows weak expression in P1–P4 of hPTC cells (L: Ladder).

selected primers were specific for PT, but also for other segments of the nephron (Table 1). Analysis started at isolated tubule/cell suspension (passage 0) used to seed the primary culture (passage 1), with the goal to determine the initial purity of the fractions (Figure 2(a)). At passage 0, all the markers analyzed in the different mixes of multiplex PCR were present in the sample, indicating the presence of all cortical nephron segments.

Cultured hPTC used for the experiments were analyzed from passages 1 to 4 (Figure 2(b)) to determine cell phenotypic stability over time. In agreement with their *in vivo* expression, RT-PCR results showed that hPTC were positive for megalin, KSP cadherin, DPPIV, SGLT-2, APN, and GGT1, all specific PT markers, at passages 1–4, indicating that these cells maintain phenotypic characteristics of PT. Also, over the four passages, NCC and NKCC2 expression was preserved, indicating either the presence of cells from others segments of the nephron, or some level of transdifferentiation. However, the expression of THP and AQP2 was lost from passage 2.

Despite MIX1 gave positive results for megalin when tested on renal tissue, this marker was not detected in cultured hPTC when analyzed as part of the MIX1. However, single RT-PCR analysis confirmed a weak megalin expression in hPTC in all passages tested (Figure 2(c)), in good agreement with its detection using alternative

techniques (ICC immunocytochemistry, see below). The RT-PCR quantification of the bands in each mix is showed as Supplementary Figure 2A.

To demonstrate the purity of our isolated hPTC, in Supplementary Figure 2B the results of a multiplex PCR analysis performed in a commercial RPTEC-TERT1 cell line were added, where specific markers from PT and other nephron segments can be identified.

### Immunofluorescence analysis of epithelial markers

The analysis of ZO-1 was performed to confirm the epithelial origin of the cells, emphasizing cell polarity. The expression of ZO-1 showed a characteristic distribution at the cell–cell boundaries (Figure 3(a)) identifying the tight junctions between the cells.

An antibody against acetylated tubulin was used to detect primary cilia. These organelles are present in polarized epithelial cells and are necessary for fluid mechanosensing-mediated regulation of tubular morphology and function.<sup>39</sup> The expression of acetylated tubulin confirmed that hPTC exhibited the primary cilium (Figure 3(b)). Thus, cultured hPTC form confluent monolayers of polarized cells, expressing tight junctions and primary cilium, both specific markers of epithelial cells, at least, until passage 3.

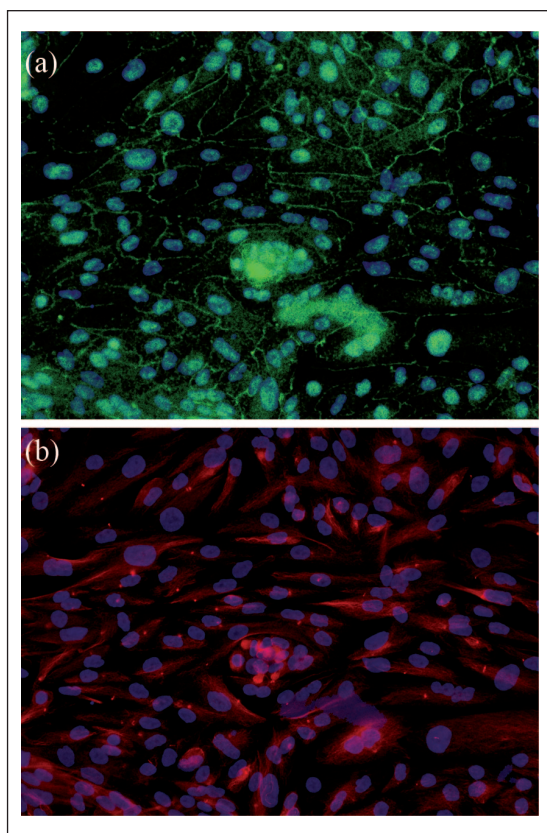


**Figure 3.** The hPTC express epithelial markers. Immunofluorescence analysis of hPTC cells seeded on coverslips, 7 days after seeding. Cells were analyzed at passage 3. (a) Expression of epithelial marker ZO-1 confirmed the formation of tight junctions. (b) The analysis of acetylated tubulin showed the expression of primary cilia (brighter dots in red).

### Immunocytochemistry characterization

Other markers with predominant cytosolic expression were assessed by immunocytochemistry in fixed cells. Expression of specific markers for PT (GGT1 and megalin), distal tubule (CB-28), and myofibroblast ( $\alpha$ SMA) was tested in samples from the first three passages. The hPTC showed a positive and a homogeneous expression for GGT1 and megalin. On the other hand, the expression of CB-28 in hPTC was weakly positive in some cells. The expression of  $\alpha$ SMA was confirmed over the cell passages. These results confirmed that the hPTC constituted of a partly heterogeneous population because despite positive PT-specific markers, markers representative for other cell types were also present (Figure 4).

### Flow cytometry analysis

Flow cytometry was used to analyze the relative expression of three specific markers with extracellular epitopes

expressed in the brush border of PT cells: CD13 (APN), CD10 (common acute lymphocytic leukemia antigen (CALLA)), and CD26 (DPPIV). We found that  $86.2\% \pm 7.6\%$  of hPTC cells were positive for CD13,  $98.7\% \pm 0.8\%$  for CD26, and  $62.0\% \pm 1.5\%$  for CD10. Importantly,  $82.6\% \pm 6.8\%$  of hPTC were simultaneously labeled for CD13/CD26 (Figure 5(a)), and  $61.1\% \pm 0.14\%$  of hPTC were simultaneously labeled for CD13/CD26/CD10 (Figure 5(b)), which confirmed the PT phenotype of most of hPTC cells.

### PT-specific enzyme activities in hPTC

The activity of two enzymes selectively expressed at the PT, GGT1, and DPPIV was quantified for this article in a high cell passage (P3) of our hPTC by measuring the liberation rate of p-nitroaniline from specific substrates. GGT1 activity, determined as p-nitroaniline liberation from GGpN in the presence of Gly-Gly, was  $110 \pm 27$  mmol/h/cm<sup>2</sup> (mean  $\pm$  SD; n=23) (Figure 6). This activity was similar to that observed in a hepatocyte cell line and several fold over the background activity observed in a mesenchymal cell line (data not shown). Data about the GGT1 activity throughout cell passages were also showed in Supplementary Figure 4.

For DPPIV, the activity in hPTC was determined to be  $83.9 \pm 16$  mmol/h/cm<sup>2</sup> (mean  $\pm$  SD; n=4). These results demonstrate the presence of functional GGT1 and DPPIV, specific enzymes for PT cells, in our isolated hPTC.

### Drug transporter assays

Presence of organic ion transporters is a main characteristic of PT cells, highly relevant in studies of drug disposition and nephrotoxicity screening, and was examined in hPTC cells. OAT1 activity was determined as probenecid-sensitive fluorescein uptake.<sup>40</sup> Figure 7(a) shows fluorescein uptake by hPTC cells, which was sensitive to inhibition by probenecid, indicating the functional presence of OAT1 in hPTC. Next, BCRP-mediated fluorescein efflux was determined by using an inhibitor of BCRP (Ko143). The use of this inhibitor increased threefold the retention of fluorescein (Figure 7(b)), demonstrating the presence of this transporter in hPTC as well.

The activity of P-gp and MRP transporters was determined by measuring the retention of Calcein in the presence of specific transporter inhibitors. To this end, hPTC cells were incubated with calcein-AM in the presence of inhibitors MK571 (MRP) and PSC833 (P-gp), respectively. As shown in Figure 7(c), an increase in the



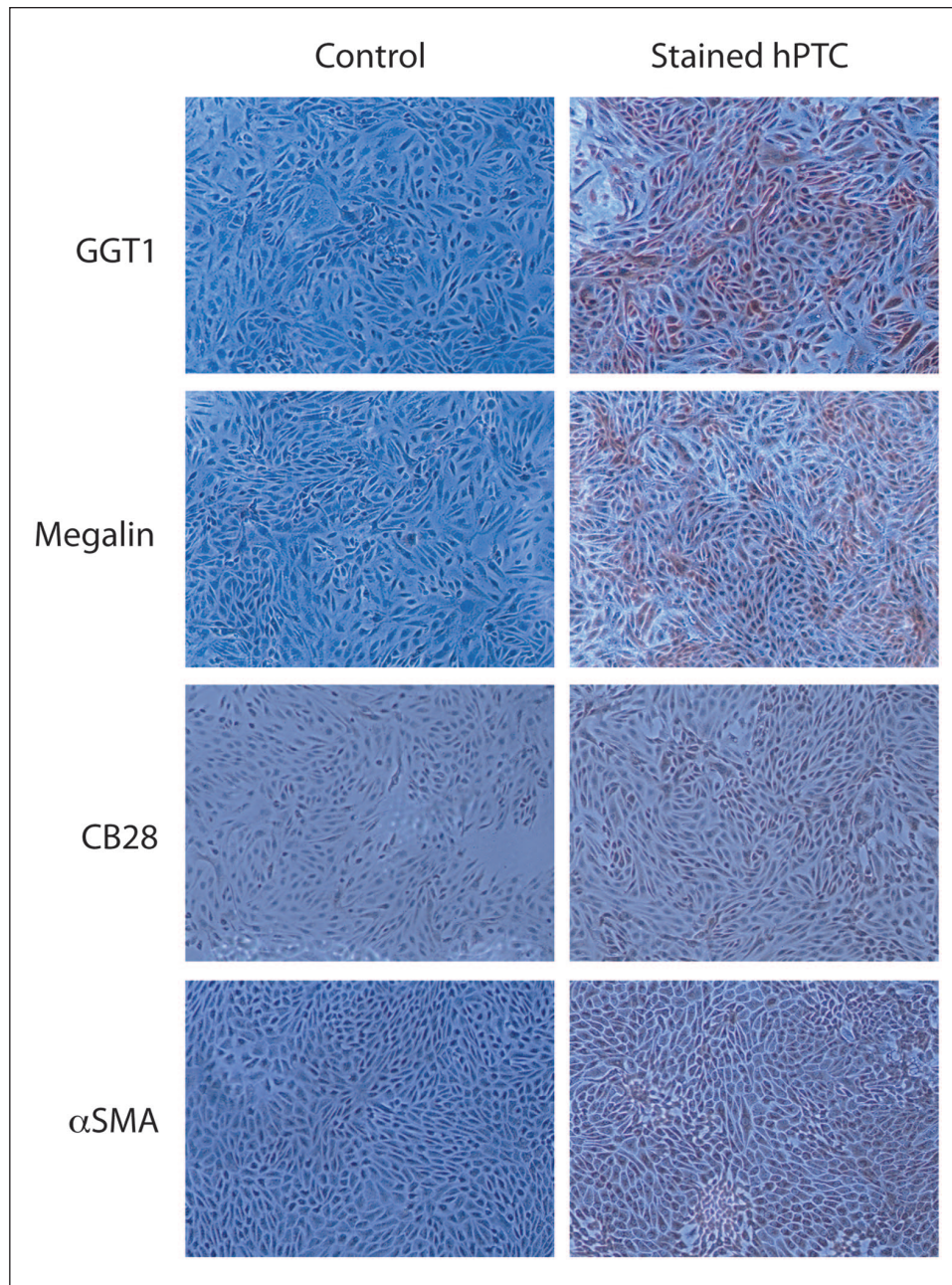


**Figure 4.** The hPTC expression of putative protein markers. Representative images of immunocytochemical analysis performed at passage 3. The expression of brush border markers GGT1 and megalin was highly positive compared with the control and confirmed that hPTC maintain the proximal tubular phenotype. The expression of CB-28, a distal nephron marker, was weakly positive compared with the control. The marker  $\alpha$ SMA is a specific marker for myofibroblast. Its presence in hPTC indicates partial transition to a mesenchymal phenotype. The quantification of the immunocytochemical analysis is shown in Supplementary Figure 3.

fluorescence intensity was observed when cells were incubated with calcein-AM, indicating that the molecule penetrated the cell membrane and was converted into the fluorescent calcein. The use of inhibitors promoted the intracellular accumulation of calcein. MK571, an inhibitor of MRP, increased the fluorescence

intensity in a ratio of 1.98. PSC833, an inhibitor of P-gp, increased the accumulation of fluorescence in a ratio of 1.70 as compared with the substrate in the absence of inhibitors. These results confirmed the functional presence of MRP and Pgp transporter activity in hPTC cells.

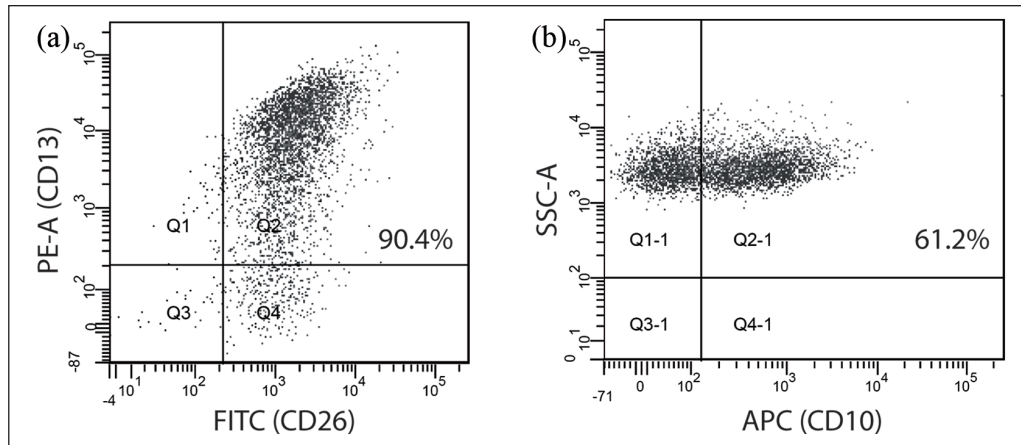


**Figure 5.** Expression of proximal tubule surface markers in hPTC. (a) Representative analysis by flow cytometry of specific markers of proximal tubule. More than 82% of hPTC were double positive for markers CD26 and CD13. (b) The double positive cell population identified in the image A was subsequently analyzed for CD10 expression, displaying 61.2% of triple positive cells.

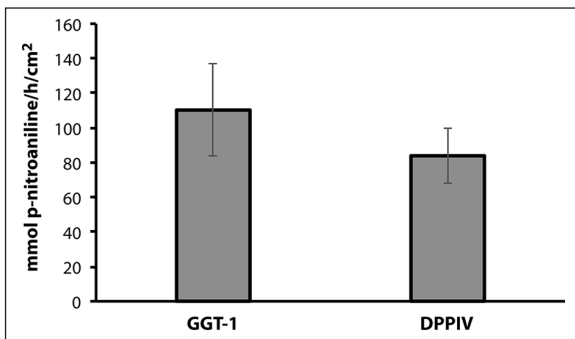


**Figure 6.** Activity of proximal tubule brush border enzymes GGT1 and DPP-IV in hPTC. GGT1 and DPP-IV activity were determined by measuring the p-nitroaniline liberated from the chemical substrates GGpN ( $n=23$ ) and GPpN ( $n=4$ ) respectively, after 60-min incubation. Data shown as mean  $\pm$  SD.

## Discussion

There is an unmet need for the culture of large numbers of differentiated PT cells that can be used in biomedical studies or to seed BAK devices. Here, we describe a simple, cost-effective, and robust method to isolate PT cells from human nephrectomies and for the simple and quick in-depth characterization of hPTC cultures.

The method we propose is based on a slightly modified isolation protocol involving selective sieving of enzymatically dissociated cells. We did not include immunoseparation techniques because they are not cost-effective. They yield lower cell numbers and use expensive reagents. With regard to preservation of PT phenotype, it is sometimes difficult to ascertain the quality of the produced materials since many reports fail to provide adequate information on the expression of non-epithelial markers or markers from non-PT nephron segments<sup>33,35,36,41–44</sup> or are not compared

to the phenotype of the starting material.<sup>12,33,41,45–50</sup> Our study shows detailed phenotypic characterization, from the initial isolated cells to the resulting cultures, performed by using specific markers from PT segment, as well as markers from other segments of the nephron. PT phenotype was also evaluated by using different independent techniques, including morphological identification, RT-PCR, immunofluorescence, immunocytochemistry, cytochemical staining, FACS, functional assays, and drug transporters assays. We put particular emphasis in not only demonstrating transcript or protein expression, but also the conservation of enzyme and membrane transport activities that are instrumental for clinically relevant PT functions. We also designed a quick phenotypic profiling tool, based on multiplex RT-PCR, that allows us for quick and cost-effective identification of changes in expression of relevant markers.

Samples from human origin, obtained from altruistic donations, are valuable and are not always readily available. Thus, our protocol also focuses in optimizing the exploitation of the obtained cells, through sequential amplification and freezing of culture aliquots. We observed that the hPTC retained their PT epithelial phenotype and doubling time capacity after thawing, for at least two passages (P2–P3). Previous publications have reported the maintenance of human primary PT cells in culture up to passage 7<sup>33,35,51</sup> although evidence is generally not documented. Despite our primary cultures lose some phenotypic characteristics at passage 4 and appear to reach senescence, it ought to be taken into consideration that we have a first amplification step, where cells probably undergo several doublings. Commercial sources report the phenotype can be maintained for 10–15 doublings, which is similar to what we calculated for our cultures. In summary, we demonstrate our method yields

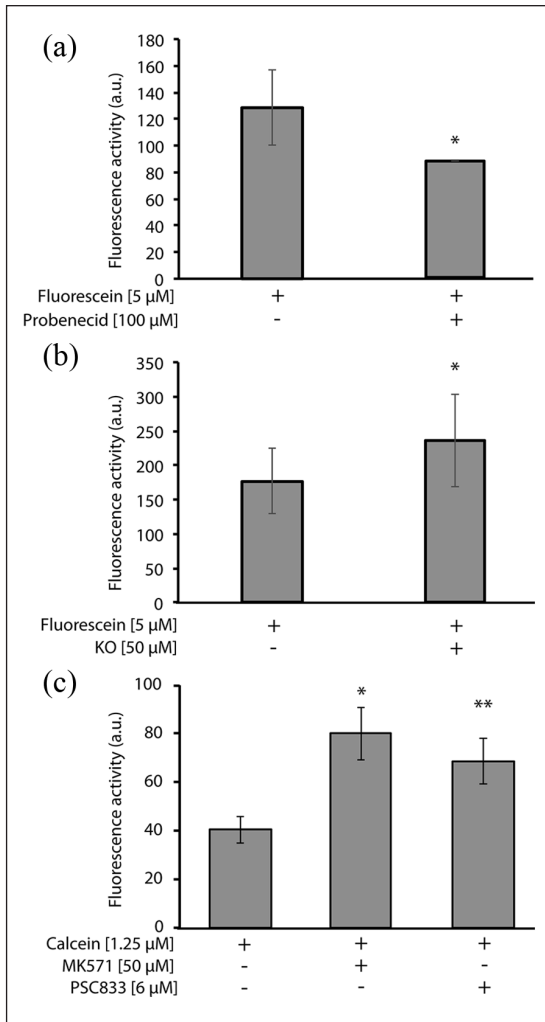


**Figure 7.** Drug transporter activity in hPTC. (a) Fluorescein accumulation in hPTC is decreased in the presence of probenecid, an inhibitor of OAT1 (n=3). (b) Fluorescein accumulation in hPTC is increased in the presence of Ko143 inhibitor, suggesting fluorescein leaves the cells through BCRP (n=2). (c) Calcein uptake was increased in the presence of MRP (MK571) and P-gp (PSC833) inhibitors, indicating these transporters are active in hPTC (n=4). Data are expressed as mean ± SD.

\*p < 0.05; \*\*p < 0.001 (two-tailed t-test).

enough cells that can be biobanked and subsequently used in two different passages. This allows for flexible experimental design and optimal use of the donated material.

The analysis of the results confirmed sustained and stable expression of PT putative markers in hPTCs. Expression of markers from other segments of the nephron (NCC—distal convoluted tubule; NKCC2—thick ascending limb of the loop of Henle; and CB-28—collecting duct) and the myofibroblast marker αSMA suggested the presence of heterogeneous cell populations. However, we did not observe the formation of

colonies with different morphologies, and microscopy analysis revealed the expression of different markers in the same cells. Thus, the most likely explanation is that conventional culture conditions select for cells with a degree of dedifferentiation or even transdifferentiation.<sup>52,53</sup> Similar observations have been reported previously and appear to be an unavoidable pay-off for achieving the proliferation required to obtain large number cells. On the other hand, we demonstrate that, together with well-known PT epithelium markers, hPTC exhibit strong brush-border enzymatic activity characteristic of PT in vivo, which is conserved through passaging of the cells. The presence of probenecid-sensitive influx of fluorescein in hPTC suggests the conservation of OAT1 activity,<sup>54,55</sup> an organic anion transporter which is used by PT cells to take up anionic drugs and toxins from blood. Transepithelial secretion relies further on transport of intracellularly captured substances through the luminal membrane. Our results demonstrate the efflux of different substrates (calcein-AM, calcein, and fluorescein) is reduced in the presence of several known inhibitors of efflux pumps. We have thus demonstrated hPTC exhibit measurable activity of several of the main organic ion transport systems (BCRP, MRP, and P-gp) required for drug and toxin secretion, hence making them a suitable model for studies of drug and toxin handling and their effects on the PT. Even if the primary focus of a study involving PT primary cultures was not nephrotoxicity, determination of organic ion pathways should be included in the phenotypic characterization, since this is a feature that has been shown to be poorly conserved in most examples of primary culture protocols or continuous cell lines derived from PT.<sup>45,56–58</sup>

We have described a simple and cost-effective method to procure large numbers of renal primary cultured cells highly enriched with PT phenotypic characteristics. This model constitutes a powerful tool for future in vitro studies in renal physiology, pathology, pharmacology, toxicology, and regenerative nephrology, where still exists a demand for PT representative cell sources, because the PT cell lines available lack important characteristics of the original tissue. Moreover, it is important to highlight that these cells could constitute a valuable tool in the development of alternative renal function replacement therapies like BAKs. Patients suffering from ESRD need novel therapies to ameliorate their health and quality of life. Currently, new strategies as the use of BAK are really promising options for these patients,<sup>14</sup> because it will replace essential renal functions, and excrete waste products actively, by using PT-like cells seeded on hollow fiber membranes.<sup>59</sup> PT cells are specialized in the excretion of xenobiotics and endogenous waste products from metabolism<sup>16,17</sup> and importantly, these types of cells promote the excretion of protein-bound uremic toxins that constitute excretion products not eliminated by standard dialysis treatment.<sup>60,61</sup> In this context, the

methods described herein to isolate, biobank, and characterize hPTC are an appealing alternative to provide a source of cells for this type of technologies.

### Acknowledgements

We want to acknowledge the technical assistance of M<sup>a</sup> Pilar Torcal and the staff of the Central Research Services from Instituto Aragonés de Ciencias de la Salud/Instituto de Investigaciones Sanitarias Aragón.

### Declaration of conflicting interests

The author(s) declared no potential conflicts of interest with respect to the research, authorship, and/or publication of this article.

### Funding

The author(s) disclosed receipt of the following financial support for the research, authorship, and/or publication of this article: This work was supported by Spain's Ministerio de Economía y Competitividad through a Grant DPI-2011-28262-C04-02 (IG) and a predoctoral fellowship BES-2012-059562 (NSR).

### ORCID iD

Ignacio Giménez  <https://orcid.org/0000-0002-6043-4869>

### Supplemental material

Supplemental material for this article is available online.

### References

- Murphy D, McCulloch CE, Lin F, et al. Trends in prevalence of chronic kidney disease in the United States. *Ann Intern Med* 2016; 165(7): 473–481.
- Delanaye P, Glasscock RJ and De Broe ME. Epidemiology of chronic kidney disease: think (at least) twice! *Clin Kidney J* 2017; 10(3): 370–374.
- Ortiz A, Covic A, Fliser D, et al. Epidemiology, contributors to, and clinical trials of mortality risk in chronic kidney failure. *Lancet* 2014; 383(9931): 1831–1843.
- Vanholder R, Baurmeister U, Brunet P, et al. A bench to bedside view of uremic toxins. *J Am Soc Nephrol* 2008; 19(5): 863–870.
- Deltombe O, VanBiesen W, Glorieux G, et al. Exploring protein binding of uremic toxins in patients with different stages of chronic kidney disease and during hemodialysis. *Toxins (Basel)* 2015; 7(10): 3933–3946.
- Jacquod A, Mathey-Doret ME, Oggier A, et al. Organ shortage: more selective waiting list requirements or an improvement in kidney donation?. *Rev Med Suisse* 2014; 10(440): 1624–1625.
- Yamanaka S and Yokoo T. Current bioengineering methods for whole kidney regeneration. *Stem Cells Int* 2015; 2015: 724047.
- Aebischer P, Ip TK, Panol G, et al. The bioartificial kidney: progress towards an ultrafiltration device with renal epithelial cells processing. *Life Support Syst* 1987; 5(2): 159–168.
- Tasnim F, Deng R, Hu M, et al. Achievements and challenges in bioartificial kidney development. *Fibrogenesis Tissue Repair* 2010; 3: 14.
- Humes HD, MacKay SM, Funke AJ, et al. Tissue engineering of a bioartificial renal tubule assist device: in vitro transport and metabolic characteristics. *Kidney Int* 1999; 55(6): 2502–2514.
- Masereeuw R and Stamatialis D. Creating a bioartificial kidney. *Int J Artif Organs* 2017; 40(7): 323–327.
- Oo ZY, Deng R, Hu M, et al. The performance of primary human renal cells in hollow fiber bioreactors for bioartificial kidneys. *Biomaterials* 2011; 32(34): 8806–8815.
- Tumlin J, Wali R, Williams W, et al. Efficacy and safety of renal tubule cell therapy for acute renal failure. *J Am Soc Nephrol* 2008; 19(5): 1034–1040.
- Humes HD, Buffington D, Westover AJ, et al. The bioartificial kidney: current status and future promise. *Pediatr Nephrol* 2014; 29(3): 343–351.
- Gekle M. Renal tubule albumin transport. *Annu Rev Physiol* 2005; 67: 573–594.
- Brown CD, Sayer R, Windass AS, et al. Characterisation of human tubular cell monolayers as a model of proximal tubular xenobiotic handling. *Toxicol Appl Pharmacol* 2008; 233(3): 428–438.
- Sanchez-Romero N, Schophuizen CM, Gimenez I, et al. In vitro systems to study nephrotoxicology: 2D versus 3D models. *Eur J Pharmacol* 2016; 790: 36–45.
- Trifillis AL. Isolation, culture and characterization of human renal proximal tubule and collecting duct cells. *Exp Nephrol* 1999; 7(5–6): 353–359.
- Toutain H and Morin JP. Renal proximal tubule cell cultures for studying drug-induced nephrotoxicity and modulation of phenotype expression by medium components. *Ren Fail* 1992; 14(3): 371–383.
- Russel FG, Masereeuw R and Van Aubel RA. Molecular aspects of renal anionic drug transport. *Annu Rev Physiol* 2002; 64: 563–594.
- Kleinman HK, Graf J, Iwamoto Y, et al. Role of basement membranes in cell differentiation. *Ann N Y Acad Sci* 1987; 513: 134–145.
- Pienta KJ, Murphy BC, Getzenberg RH, et al. The effect of extracellular matrix interactions on morphologic transformation in vitro. *Biochem Biophys Res Commun* 1991; 179(1): 333–339.
- Terryn S, Jouret F, Vandenabeele F, et al. A primary culture of mouse proximal tubular cells, established on collagen-coated membranes. *Am J Physiol Renal Physiol* 2007; 293(2): F476–F485.
- Volpe DA. Application of method suitability for drug permeability classification. *AAPS J* 2010; 12(4): 670–678.
- Ni M, Teo JC, Ibrahim MS, et al. Characterization of membrane materials and membrane coatings for bioreactor units of bioartificial kidneys. *Biomaterials* 2011; 32(6): 1465–1476.
- Schindler M, Ahmed I, Kamal J, et al. A synthetic nanofibrillar matrix promotes in vivo-like organization and morphogenesis for cells in culture. *Biomaterials* 2005; 26(28): 5624–5631.
- Sirich TL, Aronov PA, Plummer NS, et al. Numerous protein-bound solutes are cleared by the kidney with high efficiency. *Kidney Int* 2013; 84(3): 585–590.

28. Sung JH and Shuler ML. Microtechnology for mimicking in vivo tissue environment. *Ann Biomed Eng* 2012; 40(6): 1289–1300.
29. Tehranirokh M, Kouzani AZ, Francis PS, et al. Microfluidic devices for cell cultivation and proliferation. *Biomicrofluidics* 2013; 7(5): 51502.
30. Andersen KJ, Maunsbach AB and Christensen EI. Biochemical and ultrastructural characterization of fluid transporting LLC-PK1 microspheres. *J Am Soc Nephrol* 1998; 9(7): 1153–1168.
31. Ryan MJ, Johnson G, Kirk J, et al. HK-2: an immortalized proximal tubule epithelial cell line from normal adult human kidney. *Kidney Int* 1994; 45(1): 48–57.
32. Minuth WW, Strehl R and Schumacher K. *Tissue engineering: essentials for daily laboratory work*. Weinheim: Wiley Publisher, 2005.
33. Van der Hauwaert C, Savary G, Gnemmi V, et al. Isolation and characterization of a primary proximal tubular epithelial cell model from human kidney by CD10/CD13 double labeling. *PLoS ONE* 2013; 8(6): e66750.
34. Lindgren D, Bostrom AK, Nilsson K, et al. Isolation and characterization of progenitor-like cells from human renal proximal tubules. *Am J Pathol* 2011; 178(2): 828–837.
35. Baer PC, Nockher WA, Haase W, et al. Isolation of proximal and distal tubule cells from human kidney by immunomagnetic separation. *Kidney Int* 1997; 52(5): 1321–1331.
36. Van der Biest I, Nouwen EJ, Van Dromme SA, et al. Characterization of pure proximal and heterogeneous distal human tubular cells in culture. *Kidney Int* 1994; 45(1): 85–94.
37. Taub M. Primary kidney proximal tubule cells. *Methods Mol Biol* 2005; 290: 231–247.
38. Van de Water FM, Boleij JM, Peters JG, et al. Characterization of P-glycoprotein and multidrug resistance proteins in rat kidney and intestinal cell lines. *Eur J Pharm Sci* 2007; 30(1): 36–44.
39. Raghavan V, Rbaibi Y, Pastor-Soler NM, et al. Shear stress-dependent regulation of apical endocytosis in renal proximal tubule cells mediated by primary cilia. *Proc Natl Acad Sci U S A* 2014; 111(23): 8506–8511.
40. Nieskens TT, Peters JG, Schreurs MJ, et al. A human renal proximal tubule cell line with stable organic anion transporter 1 and 3 expression predictive for antiviral-induced toxicity. *AAPS J* 2016; 18(2): 465–475.
41. Vesey DA, Qi W, Chen X, et al. Isolation and primary culture of human proximal tubule cells. *Methods Mol Biol* 2009; 466: 19–24.
42. Cummings BS, Lasker JM and Lash LH. Expression of glutathione-dependent enzymes and cytochrome P450s in freshly isolated and primary cultures of proximal tubular cells from human kidney. *J Pharmacol Exp Ther* 2000; 293(2): 677–685.
43. Trifillis AL, Regec AL and Trump BF. Isolation, culture and characterization of human renal tubular cells. *J Urol* 1985; 133(2): 324–329.
44. Van Kooten C, Lam S and Daha MR. Isolation, culture, characterization and use of human renal tubular epithelial cells. *J Nephrol* 2001; 14(3): 204–210.
45. Jang KJ, Mehr AP, Hamilton GA, et al. Human kidney proximal tubule-on-a-chip for drug transport and nephrotoxicity assessment. *Integr Biol (Camb)* 2013; 5(9): 1119–1129.
46. Grabias BM and Konstantopoulos K. Epithelial-mesenchymal transition and fibrosis are mutually exclusive responses in shear-activated proximal tubular epithelial cells. *FASEB J* 2012; 26(10): 4131–4141.
47. Presnell SC, Bruce AT, Wallace SM, et al. Isolation, characterization, and expansion methods for defined primary renal cell populations from rodent, canine, and human normal and diseased kidneys. *Tissue Eng Part C Methods* 2011; 17(3): 261–273.
48. Kroening S, Neubauer E, Wullich B, et al. Characterization of connective tissue growth factor expression in primary cultures of human tubular epithelial cells: modulation by hypoxia. *Am J Physiol Renal Physiol* 2010; 298(3): F796–F806.
49. Price KL, Hulton SA, Van't Hoff WG, et al. Primary cultures of renal proximal tubule cells derived from individuals with primary hyperoxaluria. *Urol Res* 2009; 37(3): 127–132.
50. Wieser M, Stadler G, Jennings P, et al. hTERT alone immortalizes epithelial cells of renal proximal tubules without changing their functional characteristics. *Am J Physiol Renal Physiol* 2008; 295(5): F1365–F1175.
51. Detrisac CJ, Sens MA, Garvin AJ, et al. Tissue culture of human kidney epithelial cells of proximal tubule origin. *Kidney Int* 1984; 25(2): 383–390.
52. Winbanks CE, Darby IA, Kelyack KJ, et al. Explanting is an ex vivo model of renal epithelial-mesenchymal transition. *J Biomed Biotechnol* 2011; 2011: 212819.
53. Baer PC and Bereiter-Hahn J. Epithelial cells in culture: injured or differentiated cells? *Cell Biol Int* 2012; 36(9): 771–777.
54. Jansen J, Fedecostante M, Wilmer MJ, et al. Bioengineered kidney tubules efficiently excrete uremic toxins. *Sci Rep* 2016; 6: 26715.
55. Caetano-Pinto P, Janssen MJ, Gijzen L, et al. Fluorescence-based transport assays revisited in a human renal proximal tubule cell line. *Mol Pharm* 2016; 13(3): 933–944.
56. Wilmer MJ, Saleem MA, Masereeuw R, et al. Novel conditionally immortalized human proximal tubule cell line expressing functional influx and efflux transporters. *Cell Tissue Res* 2010; 339(2): 449–457.
57. Jansen J, Schophuizen CM, Wilmer MJ, et al. A morphological and functional comparison of proximal tubule cell lines established from human urine and kidney tissue. *Exp Cell Res* 2014; 323(1): 87–99.
58. Aschauer L, Carta G, Vogelsang N, et al. Expression of xenobiotic transporters in the human renal proximal tubule cell line RPTEC/TERT1. *Toxicol In Vitro* 2015; 30(1 Pt A): 95–105.
59. Jansen J, Fedecostante M, Wilmer MJ, et al. Biotechnological challenges of bioartificial kidney engineering. *Biotechnol Adv* 2014; 32(7): 1317–1327.
60. Legallais C, Kim D, Mihaila SM, et al. Bioengineering organs for blood detoxification. *Adv Healthc Mater* 2018; 7: e1800430.
61. Mihajlovic M, Van den Heuvel LP, Hoenderop JG, et al. Allostimulatory capacity of conditionally immortalized proximal tubule cell lines for bioartificial kidney application. *Sci Rep* 2017; 7(1): 7103.